EPA/600/R-17/370 | September 2017
www.epa.gov/homeland-security-research

United States
Environmental Protection
Agency

Plastic Scintillation Fibers for Radiological Contamination Surveys

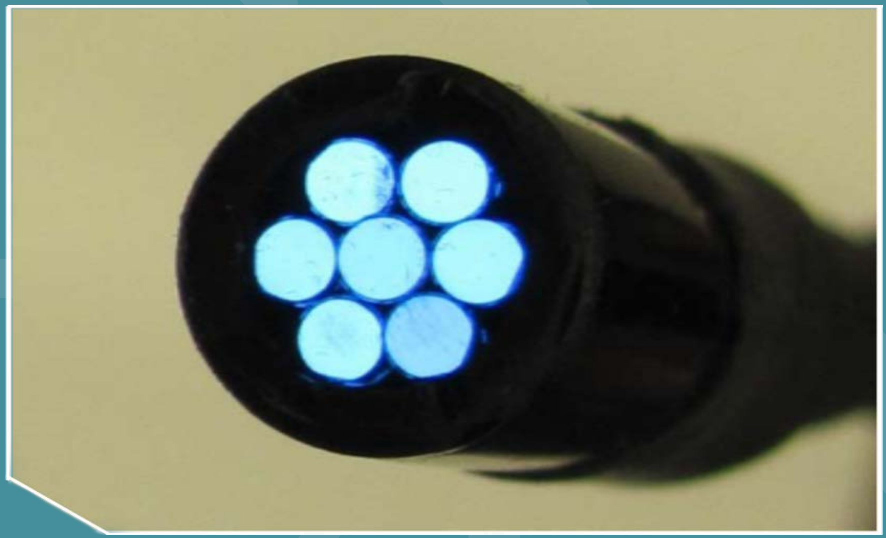

Office of Research and Development
Homeland Security Research Program

EPA/600/R-17/370
September 2017

Plastic Scintillation Fibers for Radiological Contamination Surveys

U.S. Environmental Protection Agency
Cincinnati, OH 45268

Disclaimer

The U.S. Environmental Protection Agency (EPA), through its Office of Research and Development's National Homeland Security Research Center, funded and managed this evaluation. The document was prepared by Lawrence Livermore National Laboratory under Interagency Agreement (DW-89-92426601). This document was reviewed in accordance with EPA policy prior to publication. Note that approval for publication does not signify that the contents necessarily reflect the views of the Agency. Mention of trade names or commercial products does not constitute endorsement or recommendation for use of a specific product.

Questions concerning this document or its application should be addressed to:

Dr. Sang Don Lee
U.S. Environmental Protection Agency
109 T.W. Alexander Drive
Mail Code: E343-06
Research Triangle Park, NC 27709
Lee.Sangdon@epa.gov
919-541-4531

Executive Summary

Plastic scintillation fiber (PSF) was developed and initially tested over five decades ago and has since been used to detect neutrons, x-rays and gamma-rays, track charged particles, and characterize particle beams in areas ranging from cancer treatment to wide area monitoring. PSF offers an alternative to traditional gamma-surveying techniques to survey contaminated surfaces. The advantageous features of PSF include long length, flexibility, the ability to conform to different shapes, water-/weather-proof application, and relatively inexpensive to manufacture. When combined with other pre-existing technologies, PSF can be a useful addition to the survey and remediation toolbox in responding to wide-area radiological contamination. Specifically, pairing PSF with vehicles to survey, stabilize and mark radioactive surfaces for subsequent decontamination would be of great benefit to responders. Surveying high-rise buildings to identify surfaces needing decontamination and to subsequently monitor decontamination progress would greatly improve the restoration of such buildings. Potential applications also include deploying arrays of PSF bundles to monitor and survey reservoirs and subsurface radioactive plumes. Collaboration with Japanese researchers at Japan Atomic Energy Agency is recommended to leverage PSF technology development and diverse contaminated surfaces resulting from the deposition of radioactive material from the Fukushima Dai-ichi Nuclear Power Plant disaster in 2011.

In this study, a prototype radiation detection system has been built employing plastic scintillation fiber optics. The system incorporates commercial off-the-shelf technology to display a waterfall plot showing dose rate along the 10-meter long fiber bundle. The main components are the scintillating fiber, two photomultiplier tubes (PMTs) to detect the scintillation light, a digital oscilloscope to digitize the PMT signals, a Raspberry Pi computer to perform calculations, and an Android tablet to display the data and provide a user interface. The parts for the system cost under $5,000.

The position resolution of the system is 47 centimeters (cm) full-width at half maximum (FWHM), which allows the determination of point source locations to within a few cm during a several second integration time. The fiber is sensitive to gamma rays above approximately 150 kiloelectron volts (keV) and to beta-emitting isotopes with end point energies greater than 500 keV. This range covers a large portion of radioisotopes of possible interest for decontamination. If the bundle were on a boom in front of a vehicle, a speed of 2 miles per hour would allow surveys with a sensitivity of 10 microrem per hour above typical backgrounds, allowing large areas to be surveyed quickly. The system has also been tested with the fiber submerged in water, and performance was maintained, which is potentially of interest for water infrastructure protection.

Acronyms

µCi	microcurie
µR	microrem
BNC	Bayonet Neill–Concelman
BNCT	Boron neutron capture therapy
CERN	European Organization for Nuclear Research
cm	centimeter(s)
cm^3	cubic centimeter(s)
DHS	Department of Homeland Security
DOD	U.S. Department of Defense
DOE	U.S. Department of Energy
EPA	U.S. Environmental Protection Agency
FWHM	Full-width, half-maximum
g	gram(s)
GAO	Government Accountability Office
GIS	Geographic Information System
GPS	Global Positioning System
GSPS	Giga-samples per second
h	hour(s)
HV	High voltage
IND	Improvised nuclear device
JAEA	Japan Atomic Energy Agency
keV	kiloelectron volt(s)
LLNL	Lawrence Livermore National Laboratory
m	meter(s)
m^2	square meter(s)
MCA	Multichannel analyzer
MeV	Megaelectron volt(s)
mm	millimeter(s)
mph	mile(s) per hour
mR	millirem
nm	nanometer(s)
ns	nanosecond(s)
N/A	not applicable
NPP	Nuclear power plant
PA	Preamplifier
PMMA	Poly(methyl methacrylate)
PMT	Photomultiplier tube
PSF	Plastic scintillation fiber
PSI	Paul Scherrer Institut
RDD	Radiological dispersal device
SD	Signal divider
SMA	SubMiniature version A
SUV	Sports utility vehicle

USB	Universal Serial Bus

Table of Contents

Figures

Tables

1. Introduction

After the detonation of a radiological dispersal device (RDD), improvised nuclear device (IND) or accidental radiological release from a nuclear facility such as a nuclear power plant (NPP), radioactive contamination may be dispersed over a wide area. Surveying and characterization of the radionuclides of interest, their activity and the geographical/topological distribution is vital for understanding the stabilization and decontamination that may be necessary. Monitoring is also needed during decontamination to evaluate progress and after decontamination decisions.

Land surveys can be either aerial or ground-based, each approach having pros and cons. Aerial mapping of the contamination can cover large areas quickly and is not dependent on road/terrain. However, aerial surveys do not have the same precision in area that ground-based surveys can provide. Conversely, performance of ground-based surveys can be slow, and ground-based surveys are limited by access to a given terrain (e.g., road or rail). Land surveys can also be performed using backpack-style meters. Several U.S. government agencies such as Department of Energy (DOE), Department of Defense (DOD), Department of Homeland Security (DHS) and Environmental Protection Agency (EPA) have survey capabilities, including ground-based detection in cars, trucks and vans, and aerial vehicles such as planes and helicopters. **Figure 1** shows examples of ground-based survey vehicles.

Figure 1. Example Mobile Survey Road Vehicles

Note: EPA radiation scanner van (left); Japan Atomic Energy Agency (JAEA) monitoring vehicle (right)

Several stand-off radiation search detectors evaluated by DHS (2013) include the FlexSpec Mobile (Bubble Technology, Inc., Ontario, Canada; left/right directionality, $260k integrated with Chevy Tahoe), iFind Compton Camera 442 (FLIR Radiation, Inc., Oak Ridge, TN, USA; two-plane measurement, truck-/trailer-mounted, $600k to $1.2M), Mobile Radiation Verification System (Innovative American Technology, Inc., Coconut Creek, FL, USA; vehicle-mounted or stand-alone 360-degree horizontal field of view, $175k without vehicle). However, these technologies specifically do not address mapping contamination on roads or freeway surfaces. Other portable systems such as Innovative American Technology, Inc.'s Rapid Deployment Radiation Verification System ($75k), SPIR-Ident Mobile Monitoring System (Mirion Technologies, Inc., Horseheads, NY, USA; $285k), Gardian Predator Portable Radiation Detection Kit (Nucsafe, Inc., Oak Ridge, TN, USA; cost unknown), Detective-200 (ORTEC, Atlanta, GA, USA; $95k) and Matrix Mobile ARIS (Thermo Fisher Scientific Inc., Durham, NC, USA; cost unknown) can be deployed on vehicles. However, these portable units require a large stand-off distance and are typically used for measuring field of view, not performing down-looking surface measurements. Down-looking measurements would result in a small coverage area and would require many parallel passes to cover a road or freeway. A vehicle-based gamma-survey equipment using plastic scintillation fibers (PSFs) with close proximity to road and freeway surfaces might serve as a rapid survey tool. In this study, a prototype radiation detection system has been built, employing plastic scintillating fiber optics. The system incorporates commercial off-the-shelf technology to display a waterfall plot showing dose rate along the fiber bundle. The main components are the scintillating fiber bundle, two photomultiplier tubes (PMTs) to detect the scintillation light, a digital oscilloscope to digitize the PMT signals, a Raspberry Pi computer to perform calculations, and an Android tablet to display the data and provide a user interface. The parts for the system cost under $5,000.

2. Plastic Scintillation Fiber

2.1 Plastic Scintillation Fiber Development, Theory and Recent Applications

Plastic Scintillation Fibers were developed and initially tested over five decades ago (e.g., Reynolds and Condon, 1957; Jopson, Wright and Mark, 1960; and Chupp and Forrest, 1966) largely to detect neutrons, track charged particles and characterize particle beams.

The theory of PSF is well described in Ruchti (1996), stating that the source term depends on the nature of the energy deposition, the scintillation material, the material geometry, and the path length in the material traversed by ionizing radiation. Ruchti cites Berlman (1971) in describing organic PSF and the process of excitation and transmission. Specifically, the base material (typically more than 98%) is a polymeric material such as polystyrene or polyvinyltoluene that absorbs the energy of impinging ionizing radiation, resulting in excitation of the base molecule. Since relaxation times for such polymers are slow (and, therefore, they are not good light emitters), organic fluorescent dyes can be added to the base material, and the energy can be quickly transferred from the polymer to the dye via non-radiative dipole-dipole transfer occurring on timescales less than 1 nanosecond (ns). The dye fluoresces rapidly on the nanosecond timescale, and a fraction of the visible light emitted is transmitted along the fiber itself through total internal reflection to each end of the fiber. Application of cladding with a different refractive index can prevent light loss outside the angle of total internal reflection.

Further development occurred in the 1980s and 1990s (e.g., Burmeister et al. (1984); Takasaki et al. (1987); Imai et al. (1991); Oka et al. (1998); and Ishikawa et al. (2002)) to address issues as diverse as radiotherapy cancer treatment, calorimetry, and wide area radiation monitoring.

PSFs have several key advantageous features, including (Oka et al. (1998); Park and Kim (2004); Sanada et al. (2015)):

- Long length ~20 meters (m) (urban area application)
- Flexible (durable)
- Conform to surface shape (provide improved geometry)
- High water resistance (underwater or all-weather applications)
- Can be bundled to improve detection

- Serve as both scintillator and light transmitter
- No electric power to the sensor portion is needed (less susceptible in harsh environments)
- Relatively inexpensive to manufacture
- Not influenced by magnetic fields (although PMTs are).

Two current manufacturers of plastic scintillation fiber are Saint Gobain Crystals (multinational company with Corporate headquarters located in Hiram, Ohio, USA) and Kuraray (Kuraray group corporate, Tokyo, Japan).

Saint Gobain Crystals[1] produces several different fibers (BCF-10, BCF-12 and BCF-20), each of which varies slightly in emission peak, decay time and attenuation length. The properties of each formulation are given in **Table 1**. Additionally, Saint Gobain Crystals PSF materials have operating temperatures between –20 °C and +50 °C.

Kuraray[2] produces three formulations of PSF, namely, SCSF-78 (long attenuation length and high light yield), SCSF-81 (long attenuation length) and SCSF-3HF 1500 (improved radiation hardness). Kuraray PSF products are deployed in a range of large international nuclear physics and particle tracking experiments at the European Organization for Nuclear Research (CERN). Additional properties of the Kuraray PSF are given in **Table 1**.

Fibers are also available with fluorinated polymer multilayer cladding with a lower refractive index to improve light yield by up to 50-60% over conventional single-clad fibers.

Table 1. Key Properties of Select PSF Formulations

Manufacturer	Formulation[a,b]	Emission Color	Peak Wavelength nm	Decay Time ns	Attenuation Length m	Application and Characteristics	Cost $[c]
Saint Gobain Crystals	BCF-10	Blue	432	2.7	2.2	General purpose	102
	BCF-12	Blue	435	3.2	2.7	Improved transition for long lengths	105
	BCF-60	Green	530	7	3.5	Radiation hardness	104
Kuraray	SCSF-78	Blue	450	2.8	> 4.0	Improved transition for long lengths, high light yield	N/A
	SCSF-81	Blue	437	2.4	> 3.5	Improved transition for long lengths	N/A
	SCSF-3HF	Green	530	7	> 4.5	Radiation hardness	N/A

aCommon core properties: material = polystyrene, refractive index = 1.6, density = 1.05 grams (g) per cubic centimeter (cm^3).
bCommon cladding properties: material = poly(methyl methacrylate) (PMMA), refractive index = 1.49, density = 1.19 g/cm^3.
c Comparable cost for 20 m length, 1 millimeter (mm) round diameter, single clad, non-structure oriented, spool-supplied fiber. N/A = price not available.
nm = nanometer

[1] http://www.crystals.saint-gobain.com/Scintillating_Fiber.aspx (last accessed September 2017)
[2] http://kuraraypsf.jp (last accessed September 2017)

Imai et al. (1991) detail the equations describing the interpretation of photon position from scintillation pulses observed at either end of a PSF survey system similar to the system shown in **Figure 2**.

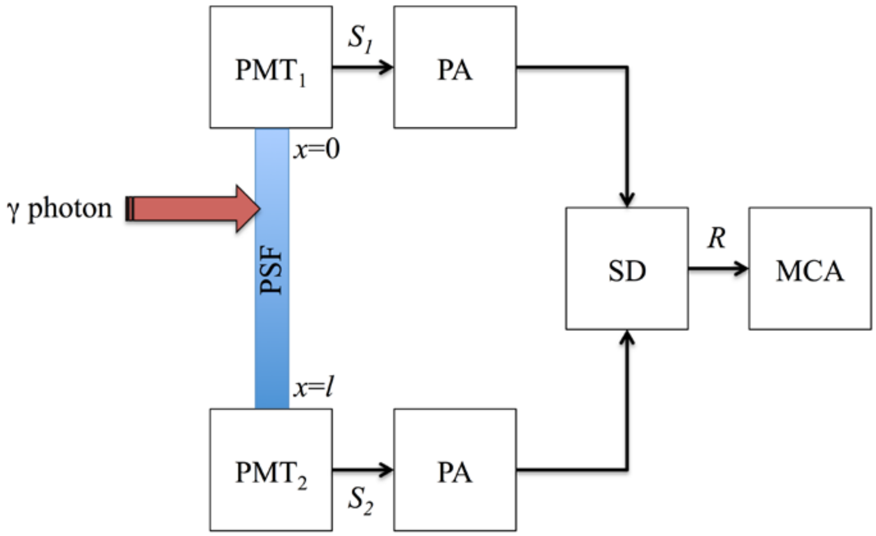

Figure 2. Simplified Schematic of a Position-Dependent PSF Gamma Survey Meter

Legend: PMT = photomultiplier tube. PA = preamplifier. SD = signal divider. MCA = multichannel analyzer.

$$S_1 = k_1 I_o \exp\left(-\frac{x}{d}\right) \text{ for PMT}_1 \qquad (1)$$

$$S_2 = k_2 I_o \exp\left(-\frac{l-x}{d}\right) \text{ for PMT}_2 \qquad (2)$$

where S_1 and S_2 are the highest of the scintillation pulses received at PMT_1 and PMT_2, respectively, I_o is the initial number of scintillation photons passing through the PSF core, k_1 and k_2 are the quantum efficiency of the PMTs, x is the scintillating position, l is the total length of the PSF and d is the attenuation length (1/e) of the PSF.

The output signal R from the divider is equal to the ratio of pulse heights at each PMT:

$$R = \frac{S_1}{S_2} = C \cdot \exp\left(-\frac{2x}{d}\right) \qquad (3)$$

where

$$C = \frac{k_1}{k_2} \cdot \exp\left(\frac{l}{d}\right) \qquad (4)$$

and

$$x = -\frac{d}{2} \cdot \ln\frac{R}{C} = -\frac{d}{2} \cdot \ln R + C \qquad (5)$$

where

$$C = \frac{1}{2}\left(l + d \cdot \ln\frac{k_1}{k_2}\right) \qquad (6)$$

The use of a logarithmic amplifier provides a linear relationship between scintillating position *x* and output signal *R*.

The attenuation length is defined as the distance along the PSF (from the point of initial excitation) when the intensity of the signal has dropped to *1/e* (36.8% of the original signal). Single fibers may not be sensitive enough to detect gamma rays, so bundling many fibers together can increase sensitivity (Park and Kim 2004). Takasaki et al. (1987) published a paper on the development and use of PSF in collaboration with Kuraray using a 2.8-m bundle of five fibers, each 1 mm in diameter to measure electrons from a ^{106}Ru source.

Imai et al. (1991) examined the properties of a 1.75 m long, 1 mm in diameter BCF-10 PSF with poly(methyl methacrylate) (PMMA) cladding to study the measurement of gamma rays, x-rays, fast neutrons and alpha particles. Alpha particles were not able to penetrate the cladding, but the results also showed the potential for spatially flexible and continuous position-sensitive detectors for neutrons, gamma rays and x-rays. Oka et al. (1998) evaluated 20-m long, 1 mm in diameter polystyrene core PSF with PMMA cladding for wide-area monitoring applications. The design included 20 m of silica fiber on each end of the PSF and found that silica fiber resulted in a decrease in the position resolution of approximately 1.5 dB/m. Resolution was measured as full-width at half maximum (FWHM) of the peak. Additional studies were performed with a 2-m length PSF to achieve a target sensitivity of 1 count per second per meter, and a bundle of ten fibers was produced, resulting in a precision of 20 centimeters (cm) or better.

Park and Kim (2004) investigated the bundles of three, seven, thirteen, eighteen and twenty-five strands of BCF-12 PSF (1 m length, 1 mm in diameter) with ^{137}Cs. The authors also investigated the effect of casing materials around the bundle (both material and thickness). More fibers resulted in increased detection efficiency. Additionally, detection efficiency was highest with aluminum, followed by PVC plastic, while the lowest efficiency was observed with stainless steel, and it was determined that an 0.8 mm aluminum casing had a much higher efficiency than a 1.2 mm aluminum casing. The authors summarize that a few strands of fibers in aluminum tubes are sensitive enough to be employed in microcurie (µCi) level environments.

Nohtomi et al. (2008) utilized a bundle of ten BCF-10 PSF elements 15 m in length and 1 mm diameter. The position resolution was estimated to be approximately 60 cm near the center of the fiber and 75 cm near the edges, again at FWHM. Good linearity was maintained between the source position and the peak channel. Nohtomi et al. point out that the use of long PSF detectors is practically limited by the significant reduction of pulse height during the propagation of the light signals inside the scintillation fiber, which is accompanied by the notable degradation of position resolution as well as counting losses.

Chichester et al. (2012) evaluated three different Saint Gobain Crystals fibers (BCF-10, BCF-12 and BCF-20), each of which varies slightly in emission peak, decay time, and attenuation length. The results showed that low-level gamma radiation fields could be detected continuously over long distances. The response was exceptionally linear over a range of lengths, including over 15 m, and the spatial resolution was typically between 50 to 60 cm, depending on fiber type and source position along the fiber. BCF-10 was found to be the most efficient of the three fibers and also provided the best spatial resolution for lengths less than 15 m, while BCF-20 performed better at lengths greater than 15 m.

In 2012, Hitachi-GE Nuclear Energy developed a plastic scintillation fiber that operates continuously for four hours with a rechargeable battery that can measure air dose rate as far as 20 m in a few seconds.[3] The work was published in 2014 (Gamo et al.), providing examples of using 1, 7 and 12 PSF bundles to measure contamination along a roadway gutter, and potential applications on a building wall, a tree, a pond and attached to a vehicle to survey roads. The technology is paired with GE's SOPHIDA and D-phod Viewer software with mesh sizes of 10 m and 1 m, respectively.

Recent work by Sanada and colleagues at JAEA has investigated the application of PSF to various contaminated areas resulting from the Fukushima Dai-ichi NPP incident. A 19-fiber, 12-meter long PSF array was placed across a field, straddling the boundary between contaminated and decontaminated land. The results showed a clear delineation between the two areas (Todani, 2011). At the same time, measurements of radiation dose rates were performed in Minamisoma City and Date City, Japan, using PSF and identifying where high doses were collocated with cracks in asphalt pavement (JAEA, 2011). Similarly, a 20-m long bundle of 10 polystyrene 1 mm in diameter PSFs with PMMA cladding was manually moved along outdoor surfaces at schools at a rate of 0.1 m/s (equivalent to 0.2 miles per hour), allowing the 2-dimensional mapping of ^{137}Cs before and after decontamination (Torii and Sanada, 2013). In the same paper, the technique was also applied to the front of a construction vehicle (e.g., IHI CL45 compact track loader) and allowed the mapping of a 2,000-square meter (m^2) area within one hour. Assuming a road lane width of 3 m, the corresponding speed of the motorized application was 0.4 miles per hour. Additional studies were documented using PSF to measure the contamination at the bottom of a pond in the Fukushima Prefecture using a 20 m submerged PSF bundle (JAEA, 2014a). An extended length (50 m) PSF was used to monitor leakage from contaminated water tanks at the Fukushima Dai-ichi NPP (JAEA, 2014b; JAEA, 2015)

Sanada et al. (2015) utilized nineteen bundled 1 mm diameter, 20 m length Kuraray SCSF-3HF PSFs to measure ^{137}Cs sediments below water in irrigation ponds that had collected falling rain in the Fukushima prefecture. The results compared well with sediment cores withdrawn after measurement with PSF. Subsequent measurements taken after decontamination were integrated with Geographic Information System (GIS) maps to demonstrate monitoring of decontamination efficacy. Example JAEA applications are shown in **Figure 3**.[4] JAEA's PSF system is a "p-Scanner" which is equipped with a PSF detector built by JREC Co. Ltd. (Eniwa City, Hokkaido, Japan) and the data processing software.

Collaboration with Japan and leveraging PSF development in contaminated environments can better prepare the U.S. radiological response capability in urban and rural areas. Potential applications have been identified, together with scientific and technical gaps that need to be addressed before development and deployment in the U.S.

---

[3] http://enformable.com/2012/05/ge-developing-fiber-optic-gamma-radiation-dose-rate-detection-and-measurement-system/ last accessed September 2017)

[4] Research and development of radiation measurements following nuclear power mechanism, Japan Atomic Energy Agency Fukushima Research and Development Department, Fukushima Environmental Safety Center, November 20, 2015 (Japanese), provided by JAEA/Sanada.

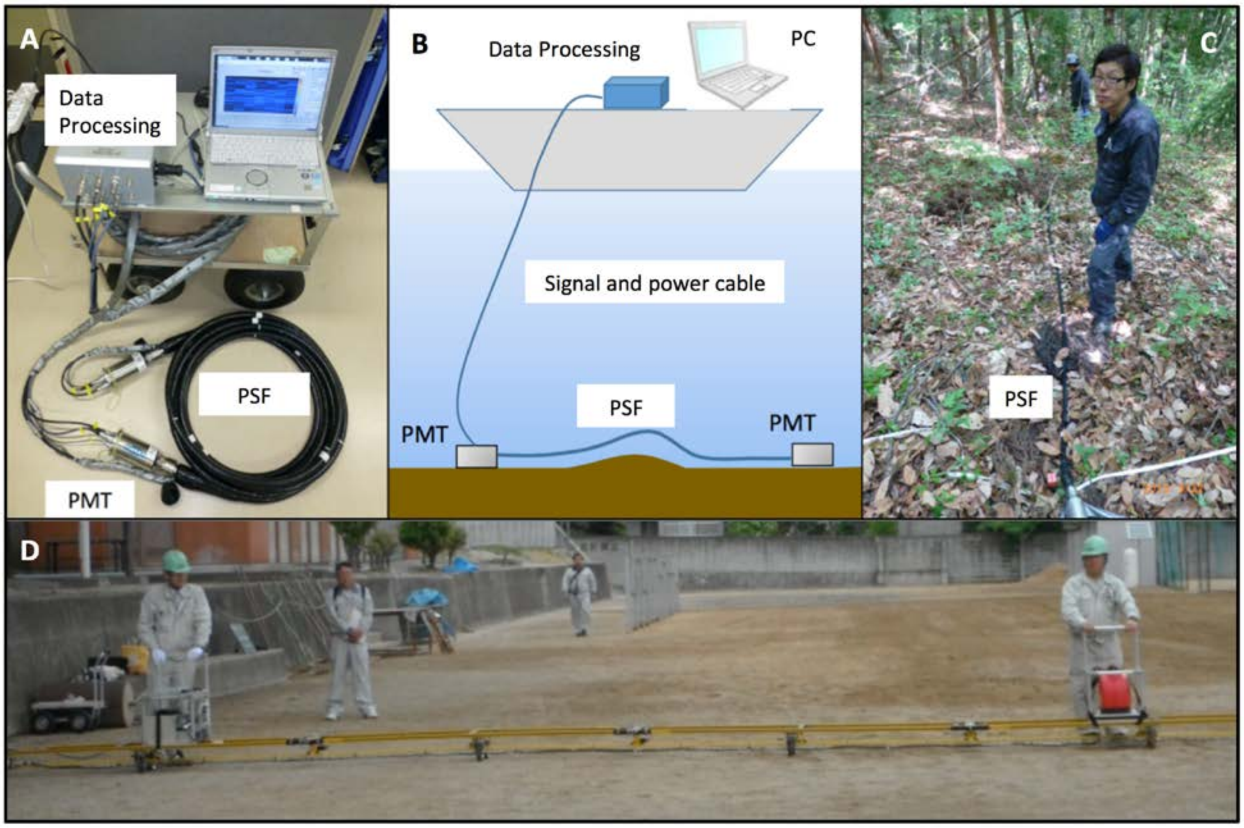

Figure 3. JAEA Application of PSF in Post-Fukushima Surveys (reproduced from JAEA[4])

(A) PSF equipment supplied by JREC Co. Ltd.; (B) Application of PSF to survey pond sediments; (C) Application of PSF to survey forest soil; (D) Application of PSF to measure outdoor urban surfaces, e.g., school playground.

2.2 Radiological Response Survey Technology Applications

2.2.1 Application in Transportation and Agriculture Sectors

As demonstrated in Japan using a compact loader (Torii and Sanada, 2013), PSF can be attached to vehicles to provide two-dimensional survey capability. The concept may be extended to include application on vehicles traveling at a higher rate of speed, for example, on a truck, van or sports utility vehicle (SUV) fitted with signal processing equipment to provide real-time ground surveys of roads and freeways, a capability additional to those already maintained by DOE, DHS, EPA[5], and JAEA[6].

According to the US Department of Transportation Federal Highway Administration[7], the recommended US freeway lane width is typically 3.6 m, and a local roadway is typically 2.7 to

[5] http://www.epa.gov/radiation/radiological-emergency-response-expertise-and-equipment#tab-2 (last accessed September 2017)

[6] Sasakino Analytical Laboratory, JAEA Fukushima Environmental Safety Center

[7] http://safety.fhwa.dot.gov/geometric/pubs/mitigationstrategies/chapter3/3_lanewidth.cfm (last accessed September 2017)

3.6 m. Therefore, for a five-lane freeway, the freeway width on either side of the median is 18 m (not including shoulder). It is therefore possible to survey the entire width of a freeway in a single pass with a 20-meter PSF perpendicular boom. In this case, the rate of surveying would be dependent on the response of the PSF with respect to vehicle speed. Alternatively, PSF perpendicular booms could be deployed that are between 2.7 and 3.6 m wide to survey single freeway lanes and local roads. Freeway on- and off-ramps are typically 3.6 to 9.2 m per lane, while arterial roads are between 3.3 and 3.6 m per lane. The outside paved shoulder width on freeways should be at least 3.0 m, while inside shoulder width should be between 1.2 and 3.0 m, depending on the number of lanes and truck traffic. Shoulders for mountainous terrain may be smaller. Similarly, the approach could be used to survey airport runways, taxiways, loading/servicing/maintenance areas. In Japan, the technology could be evaluated and demonstrated on local contaminated roads and potentially the Joban Expressway.

For agricultural land, PSF may be combined with farm equipment such as a tractor. Alternatively, when combined with a combine harvester, areas of contamination may be removed immediately. The technology may also be applied to a *work train* typically used for track maintenance. Such an application may permit surveying of track and ballast to assist in decontamination planning and waste minimization.

Proposed evaluations and demonstrations

The speed of surveying should be optimized to balance detection sensitivity with surface area and time constraints. This study will likely include a variation in PSF length and bundle size. Several vehicles should be evaluated, including: (a) the JAEA Sasakino Analytical Laboratory SUV, (b) a larger vehicle capable of accommodating a longer PSF for freeway or runway application, and (c) a rail work car. Additionally, the application of a stabilization agent, fixative or marker should also be demonstrated to aid in the decontamination planning and preparation. Such an application may require deployment on a service vehicle such as a tanker/spray/spreader truck or street-sweeping vehicle. Additionally, the speed of the vehicle should be investigated to determine the fastest speed that can still achieve detection at the appropriate level. One possible solution to increase speed and improve detection is applying fibers parallel to the vehicle motion, providing detection along the entire length (or beyond if towed). This application would require multiple bundles to cover the area beneath the vehicle. For example, if it is assumed that a single PSF at a distance of 10 cm from the surface has a viewing angle of 90° (with some collimation to prevent background from sky-shine and surroundings), a 20 cm viewing region is produced under the entire length of the fiber. A vehicle equipped with five bundles of 2 m PSF fibers spaced approximately 20 cm apart may cover a 1 m wide vehicle and may survey 2 m^2 at any given time, resulting in quicker surface scanning capabilities (potentially 2 to 10 miles per hour [mph]) compared to a single bundle placed perpendicular to the vehicle motion (such as those demonstrated by JAEA at 0.2 mph). However, axial positioning of PSF compared to the vehicle motion would result in a minimum resolution of 20 cm for survey positioning. A combination of transverse and axial fibers in a grid may provide both improvements in survey speed while maintaining the sensitivity demonstrated by Sanada et al. Rapid detection will improve the early phase response using containment or decontamination technologies.

2.2.2 Building Survey and Decontamination Progress Applications

Surveying contamination on the outside of a high-rise building may be challenging in built-up urban areas and major cities. Additionally, monitoring the progress of high-rise building decontamination without interference from ground-shine, sky-shine and background from other buildings is also problematic. One solution is to attach a PSF bundle to a window-cleaning platform (e.g., **Figure 4**)[8] and move the platform across the surface of each wall. This process would permit "mapping" of the entire building and would provide insight into decontamination methods (related to the level of contamination and the surface type and geometry). Provided a rigid casing or support is provided for the PSF, the length of the PSF could extend beyond the platform.

Figure 4. An Example Window-Cleaning Platform

Proposed Evaluation and Demonstration:

Surveying the outer walls using PSF was proposed by Gamo et al. (2014) using a hand-held long wand to survey the first two floors of a building. However, this is not practical for larger, taller buildings. PSF should be evaluated and demonstrated using a window-cleaning platform to survey high-rise buildings and to determine the need for collimation to aid in the determination of building decontamination options and also demonstrate building decontamination progress monitoring.

2.2.3 Water and Subsurface Applications

The properties of PSF permit application in submerged or wet environments. As already demonstrated by JAEA (2014a; 2014b; 2015), PSF can be used to survey the bottom of ponds and the perimeters of storage vessels. Typical sediments often bind ^{137}Cs contamination quickly, creating an equilibrium between the solid and liquid phase components of a pond. Monitoring reservoir outflow pipes can be achieved using traditional detection equipment or by taking aliquots and measuring off-line. PSF may be deployed upstream of such pipes to ensure

[8] https://en.wikipedia.org/wiki/Window_cleaner#/media/File:Platform_window_cleaner.jpg (last accessed October, 2017)

reservoir security and water quality *before* waters enter the flow control and downstream release systems.

It may also be possible to bury strings of PSFs to measure infiltrating groundwater and to map and monitor plumes of contamination. Grids of PSF bundles (for example, as large as 50 m as demonstrated by JAEA) may be deployed to detect and characterize radiological vector movement in a 3-D environment, as depicted in **Figure 5**. Aluminum or PVC plastic may be used as a casing without significant attenuation of detection (based on Park and Kim, 2004).

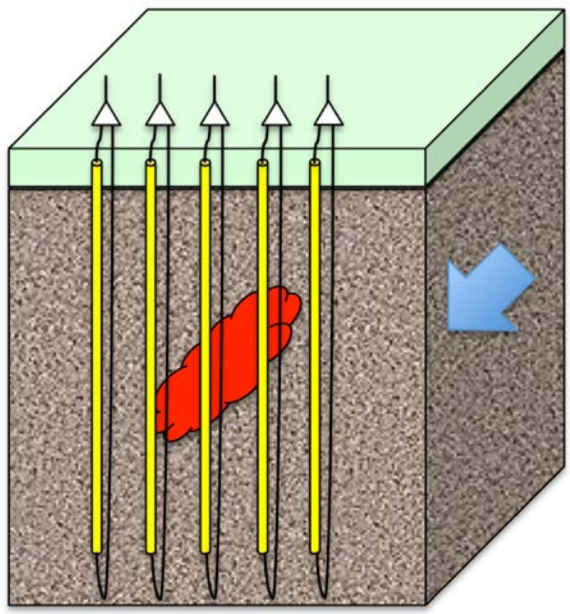

Figure 5. Schematic Diagram of Five PSF Bundles to Monitor a Subsurface Radioactive Plume

Legend: Red = plume. Blue = groundwater flow direction. Yellow = vertical PSF bundles. White = signal divider.

In each application, collimation is important. Measuring the radioactivity associated with sediment requires screening out radioactivity from the water above the sediment. Similarly, measurement of contamination on a road via deployment of PSFs on a vehicle requires removal of background signals from contamination on the vehicle itself, sky-shine or emanation from nearby contaminated surfaces. On vehicles, this removal of signal may be achieved using a semi-circular shield on the top half of the fiber, permitting scintillation in the fiber from only the radiation shining upwards from the ground. Such a shield would likely be rigid and would preclude some of the benefits of PSF (flexible and conforming to shapes). A similar situation applies for applications in monitoring decontamination progress with PSF.

Proposed Evaluations and Demonstrations:

The demonstration of PSF to survey sediments in ponds has already been accomplished by JAEA (2014a). Sediments containing clay typically sequester ^{137}Cs and incorporate the contamination into the mica sheets within the clay structure. Therefore, surveying of sediments is an extremely useful technique to understand the ^{137}Cs sequestration process from water to sediment, any potential resuspension of sediment due to currents or maritime traffic, and the sediment as a potential source for dissolution of ^{137}Cs upon changing aquatic conditions. The technology should be demonstrated on a larger scale, e.g., a reservoir. The study should assess both active (sweeping the sediment) and passive (autonomous, in-situ, real-time) monitoring. The latter deployment may require an array of PSF bundles upstream from the outflow area.

Water tower security and quality represents another potential application that requires evaluation and demonstration. Since PSF has already been demonstrated on a tank of contaminated water (JAEA, 2015), an evaluation and demonstration of application on a community water tower would require testing of sensitivity to determine low levels of contamination.

Plume monitoring (as discussed above) may be achieved when using an array of PSF bundles buried beneath the surface, downstream from the groundwater flow. Arrays may be positioned vertically (as shown in **Figure 5**) or horizontally, although the former may be more feasible to deploy. Two example demonstrations include monitoring of runoff and subsurface flow at the base of a contaminated mountain (in collaboration with JAEA and National Institute for Environmental Studies (Japan), and the monitoring of contaminated groundwater from the Fukushima Dai-ichi NPP in collaboration with Tokyo Electric Power Company.

Drinking water and wastewater are other areas of application for the PSF. Online monitoring of radiation in drinking water is difficult due to the moderating effect of water. The PSF could be put into the flow of tap water or wastewater and baseline (or background) radioactivity levels established. Short-lived radionuclides could then be spiked into the flow, which would help establish the minimum detection level of the PSF. Evaluating the effectiveness or progress of decontamination in drinking water pipes after a contamination event is another application. A water pipe could be contaminated with a short-lived radionuclide and decontamination undertaken. The PSF could be moved down the pipe between fire hydrants before and after decontamination to determine the effectiveness of the decontamination technique. In summary, the application of PSF to further assist in the survey and monitoring of contaminated surfaces, materials and water requires additional evaluation and demonstration. Such work should be performed in collaboration with experts in Japan, applying technologies to ^{137}Cs- contaminated areas resulting from the Fukushima Dai-ichi NPP release.

3. PSF Prototype

The PSF may be able to provide multiple benefits during a wide area response. The magnitude of impacted surfaces (both variety and area) may present a significant challenge and technical gap. In National Planning Scenarios, an example RDD may contaminate 36 city blocks (typically a fraction of a square mile), while an example IND may contaminate 3,000 square miles (Government Accountability Office [GAO], 2013). Technologies that can be moved across contaminated surfaces may prove to be useful tools in identifying contamination. Pre-planning for monitoring and subsequent remediation can greatly reduce the time to respond, and subsequently can minimize further contamination and reduce cleanup costs, allowing responders to minimize the impact to both public health and the environment. Roads and critical infrastructure will be of primary focus for recovery efforts in the short term (road, rail, air), providing ingress and egress routes, power, water, communications, health, security and emergency services. As addressed in Section 2, the PSF can be applied under varied situations that may be difficult for the existing detectors or monitors.

The objectives for the testing and development of PSF arrays are:

- Develop a portable detector with ease of use and applications in both roads and water infrastructure protection and recovery
- Improve hardware from the JAEA demonstration of PSF technology
- Use commercial off-the-shelf where practicable
- Provide interchangeable bundle lengths (e.g., 2 m and 10 m)
- Determine feasibility and characteristics of vehicle application to measure ground contamination.

3.1 PSF Detector Components

A PSF detector contains a specified length of plastic scintillation fiber with a known attenuation length, PMTs, a digital oscilloscope, a data communication board, and a computer controller capable of displaying and recording results. For development and testing of Lawrence Livermore National Laboratory's (LLNL) PSF detector, the following components were used:

(a) Saint Gobain Crystals BCF-12 scintillation fiber, 2-mm diameter (single and double cladding to be used separately). BCF-12 has improved transmission for longer lengths, results in a blue emission color with a 435-nm emission peak, 3.2 ns decay time, an attenuation length of 2.7 m and approximately 8,000 photons per megaelectron volt (MeV). The trapping efficiency is at least 3.4% for single clad fibers and at least 5.6% for double clad fibers.[9] The 2-mm diameter BCF-12 fiber was bundled in groups of 7 (**Figure 6**) to create a 6-mm diameter bundle. The 2017 cost was $9.20 per m for double-clad fiber when ordering 100 m or more.

    An outer sleeve is required to prevent background ambient light reaching the fibers, to maintain bundle integrity, to allow waterproofing, and to increase durability. Initial attempts at encasing the fiber bundle had used black vinyl tubing, but the thickness of the black vinyl tubing reduced the beta radiation sensitivity. Subsequently, fiber bundles were wrapped with 3M FP-301 heat-shrink tubing (polyolefin, 0.38-inch internal diameter before shrinking, 2:1 shrink ratio), allowing for a reduction in sleeve thickness by approx. 80% over vinyl tubing and resulting in greatly increased sensitivity of the fiber bundle to beta radiation. The heat-shrink tubing became somewhat stiff when shrunk, so the ends of the bundle (approximately 8 inches) were heat-shrunk to grip the fibers and maintain a fixed position in the connectors, while leaving the rest of the bundle length unshrunk to maintain flexibility. A major

[9] https://www.crystals.saint-gobain.com/sites/imdf.crystals.com/files/documents/sgc-organics-plastic-scintillators_0.pdf (last accessed January 2018)

consideration in the selection of the heat shrink tubing was finding a material with a shrinking temperature below the melting point of the plastic fibers.

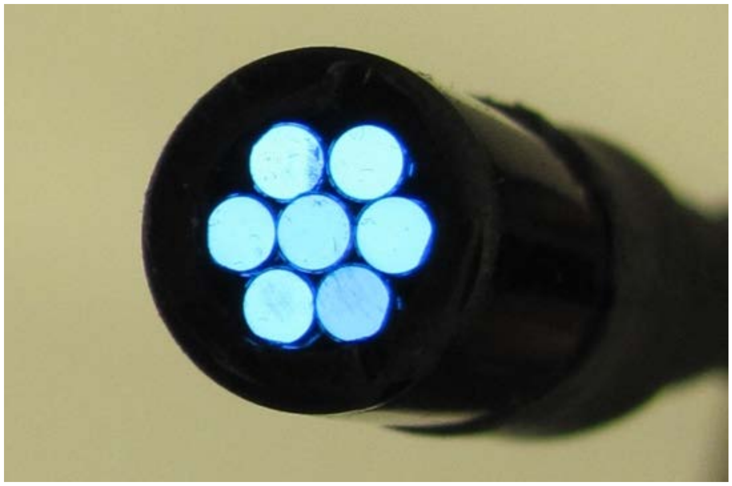

Figure 6. Bundle of Seven BCF-12 Scintillation Fibers Glowing from UV Light

(b) Two Hamamatsu 10721P-210 PMT modules with an 8-mm diameter face and built-in high voltage (HV) power supply (**Figure 7**, left panel)[10], with a 2017 cost of $980 each. Also shown in **Figure 7** (right panel) are the parts required to connect the PMT to the fiber bundle (BNC [Bayonet Neill–Concelman] Jack: Amphenol 31-203-RFX, BNC Plug: Amphenol 31-2-RFX) and the completed connection between PMT and fiber bundle. The BNC connectors were modified by drilling out the center to accommodate the fiber bundle.

Figure 7. Image of Hamamatsu 10721 PMT and Subsequent Connection to Seven-Fiber Bundle

(c) A Paul Scherrer Institut (PSI) DRS4 evaluation board four-channel digital oscilloscope using Universal Serial Bus (USB) power and communication (**Figure 8**)[11] with a 2017 cost of $1,245.

[10] http://www.hamamatsu.com/us/en/product/alpha/C/3044/H10721-20/index.html (last accessed October 2017)
[11] https://www.psi.ch/drs/evaluation-board (last accessed October 2017)

Figure 8. Image of PSI DRS4 Evaluation Board

(d) A Raspberry Pi 3 single-board computer with USB and WiFi connectivity (**Figure 9**).[12] The current typical cost is approximately $50, depending on accessories purchased. Custom software was written to interface with the DRS4 and with an Android tablet. Most computers that run Linux could be used as well.

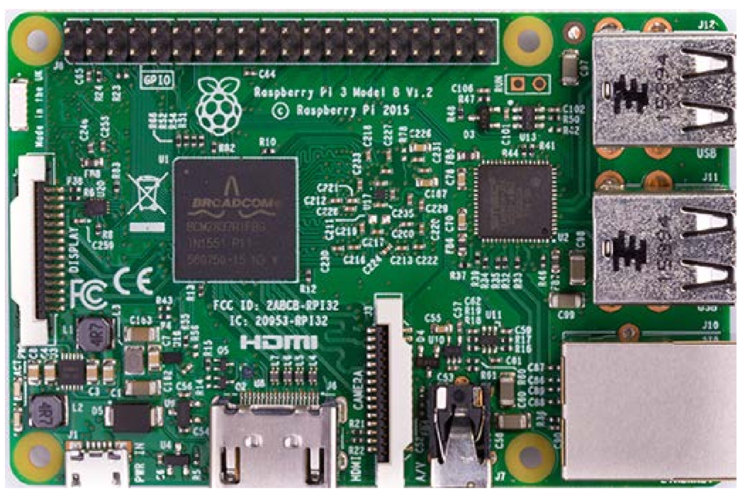

Figure 9. Image of Raspberry Pi 3 Board

(e) An Android tablet to interface with the detector system. The tablet used is a Samsung Galaxy Tab S2 (**Figure 10**)[13], which in 2017 cost approximately $250. Custom software was

[12] https://www.raspberrypi.org/products/raspberry-pi-3-model-b/ (last accessed October 2017)

[13] http://www.samsung.com/global/galaxy/galaxy-tab-s2/ (last accessed January 2018)

written to interface with the Raspberry Pi and display the dose rate along the fiber. Other Android tablets would likely work as well, as long as they run versions 4.4 to 6 of Android. Android 7 might work, but the app has not been tested with it. Note that some tablets have strong internal magnets designed for use with accessories such as keyboards, and these magnets can interfere with PMT operation.

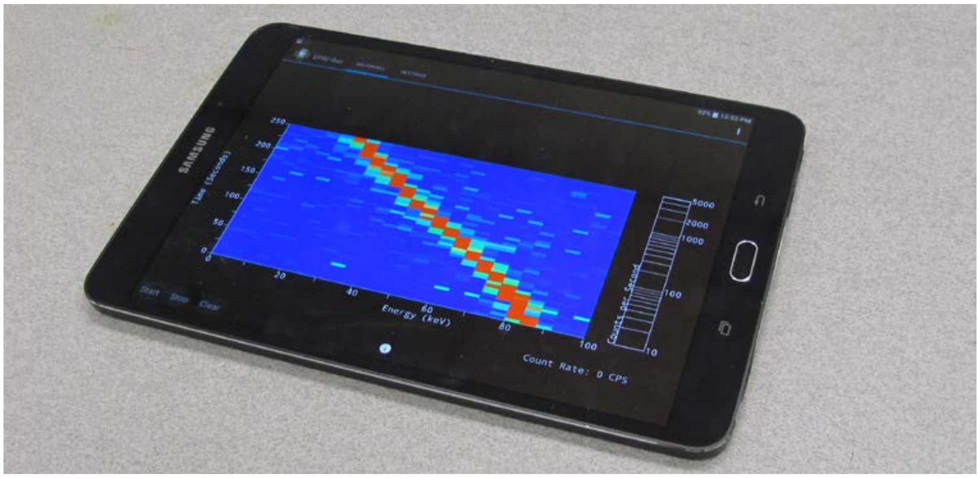

Figure 10. Samsung Galaxy Tab S2 Tablet

A schematic image of the complete system is shown in **Figure 11**, showing connections between each component, and **Figure 12** shows the prototype PSF detector system with data acquisition and tablet operation.

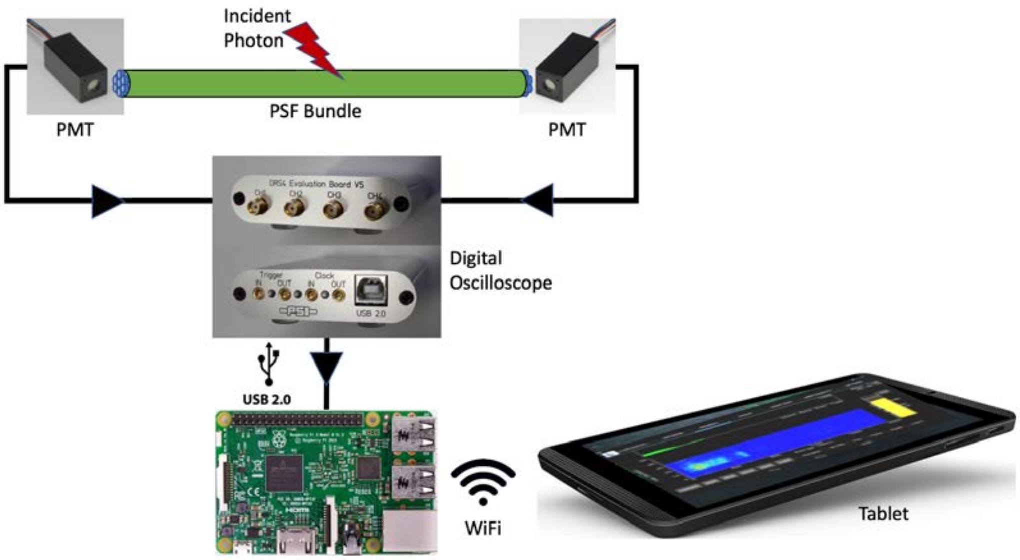

Figure 11. Schematic Diagram of the Prototype PSF Detector Components

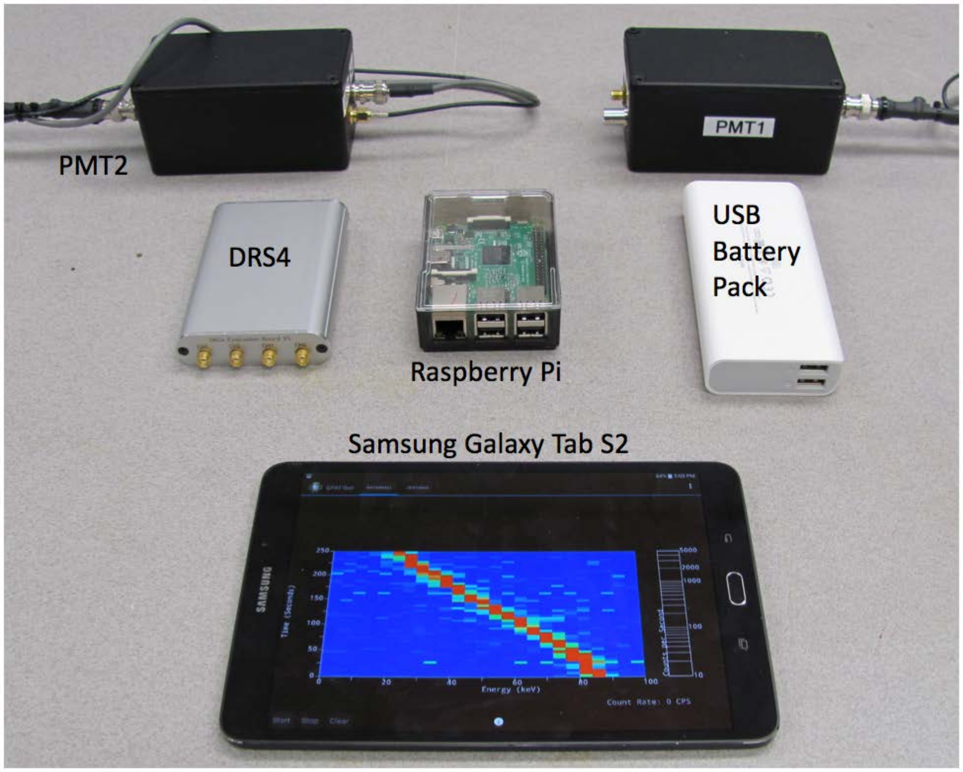

Figure 12. 7-Fiber Bundle PSF Detector System with Data Acquisition and Tablet Operation

The PSF prototype system tests were conducted by comparing the dose rate measurements using a Fluke model 451B Ion Chamber Survey Meter (**Figure 13**)[14] certified to provide readings within 10% when measuring between 20 kiloelectron volts (keV) and 2 MeV x-rays and gammas and between 0.5 millirem (mr) per hour (h) and 50 r/h. It is recalibrated annually.

Figure 13. Fluke model 451B Ion Chamber Survey Meter

---

[14] https://www.grainger.com/search?searchBar=true&searchQuery=451B+ion

3.2 PSF Detector Testing and Characterization

Radioisotope sources were used to determine the position resolution, dose rate accuracy and minimum detectable dose rate. Tests were performed with the fiber in air and also submersed in water to evaluate the performance of the ability of the detector to detect contamination on roads relevant to transportation infrastructure, and underwater relevant to water infrastructure protection and early detection. Characterization was performed using available beta and gamma radioisotope sources. In the location where the PSFs were tested, LLNL possesses the following beta sources:

- Cs-137 (514 keV beta end-point)
- Sr90/Y-90 (546 keV and 2.3 MeV beta end-points)

In the same location, LLNL possesses the following gamma sources:

- Am-241 (60 keV)
- Ba-133 (predominately 356 keV)
- Co-57 (120 keV)
- Cs-137 (662 keV)
- Co-60 (1,173 and 1,332 keV)

3.2.1 Attenuation Length

The attenuation length as provided by Saint Gobain for BCF-12 is 2.7 m. LLNL verified the attenuation length of a 7-fiber bundled PSF detector by determining the maximum intensity of photons from Cs-137 at 1 m intervals from the PMT and fitting the data points to the equation $I = I_0e^{-x/\alpha}$, where α is the attenuation length and I_0 is the maximum intensity at position 0, right next to the PMT. The attenuation length was determined to be 2.65 ± 0.1 m, consistent with the value from Saint Gobain.

3.2.2 Position Resolution

To evaluate the position resolution, the seven-fiber bundle was laid out. Collimated sources listed above were placed at several different locations along the length of the fiber. Gamma sources were collimated with lead bricks, and beta sources were collimated using plastic discs with a 3-mm hole in the center. In both cases, the aperture was much smaller than the position resolution of the system. The width of the position peak was used to determine the position resolution.

An experimental test matrix for determining position resolution is shown in **Table 2,** which was completed to determine position resolution along a fiber or fiber bundle. Position is listed as percent of the length of the bundle from one end. The test matrix was completed with peak position in percent of length and physical distance from the end, measured in centimeters and repeated in triplicate. The seven-fiber bundle used for this measurement was 10 m.

The Am-241 source, which emits 60 keV gamma rays, had too low an energy to be detected using the 10-m fiber bundle. In addition, the Co-57 source, which emits 122 keV gamma rays, has a very low detection efficiency and was barely visible above background, producing poor results due to a combination of the low light yield of plastic scintillators combined with high losses over the 10-m fiber. Both Am-241 and Co-57 were visible to 3 m and 1 m fiber bundles. To fill the energy gap between Co-57 at 122 keV and Cs-137 at 662 keV, measurements were conducted with Ba-133, which emits gamma rays predominantly at 356 keV. Measurements in **Table 2** were all for 1000 counts total along the fiber. The results show excellent position determination for energies above 350 keV. The position FWHM is 47 cm and is consistent across the length of the fiber. With 100 counts from a point source, the position is localized to within 3 cm.

Table 2. Position Resolution Test Matrix for a 10-m Seven-Fiber Bundle

Nominal Distance along fiber	10%	20%	30%	40%	50%
Actual Distance along fiber (cm)	100	200	300	400	500
Cs-137 Beta					
Rep 1	104.8	197.2	299.3	397.1	495.6
Rep 2	104.5	199.3	296.6	396.1	495.2
Rep 3	103.1	199.7	297.1	397.4	495.3
AVERAGE	104.13	198.73	297.67	396.87	495.37
STDEV	0.91	1.34	1.44	0.68	0.21
Sr-90/Y-90 Beta					
Rep 1	100.6	201.3	298.4	396.2	494.1
Rep 2	101.0	202.1	297.8	398.2	494.4
Rep 3	101.0	198.6	300.2	396.1	494.0
AVERAGE	100.87	200.67	298.80	396.83	494.17
STDEV	0.23	1.83	1.25	1.18	0.21
Am-241 Gamma	No measurable results				
Co-57 Gamma					
Rep 1	97.7	197.6	254.0	408.6	444.2
Rep 2	99.0	199.7	326.0	401.5	480.0
Rep 3	106.7	204.4	307.8	393.7	478.8
AVERAGE	101.13	200.57	295.93	401.27	467.67
STDEV	4.86	3.48	37.44	7.45	20.33
Cs-137 Gamma					
Rep 1	99.7	198.7	298.1	395.1	493.2
Rep 2	101.0	199.1	295.8	394.6	492.8
Rep 3	100.2	198.5	297.2	394.2	494.1
AVERAGE	100.30	198.77	297.03	394.63	493.37
STDEV	0.66	0.31	1.16	0.45	0.67
Co-60 Gamma					
Rep 1	99.9	198.6	295.8	393.1	493.1
Rep 2	100.5	198.6	297.8	395.6	494.3
Rep 3	100.9	199.2	296.4	393.2	494.3
AVERAGE	100.43	198.80	296.67	393.97	493.90
STDEV	0.50	0.35	1.03	1.42	0.69
Ba-133 Gamma					
Rep 1	101	200.7	297.4	394	490.6
Rep 2	104.4	199.4	298.8	395.7	492.1
Rep 3	103.2	201.2	295.9	396	490.3
AVERAGE	102.87	200.43	297.37	395.23	491.00
STDEV	1.72	0.93	1.45	1.08	0.96

Measurements were also made with an individual fiber 15 m in length for one beta and one gamma source (**Table 3**). The test matrix was completed with peak position in percent of length and physical distance from the end, measured in centimeters and repeated in triplicate. The measurements were all made for 1000 total counts in the fiber. The position FWHM is 55 cm for the 15-m bundle.

Table 3. Position Resolution Test Matrix with Replicates in Parentheses for a 15-m Single Fiber

Source / Radiation					
Nominal Distance along fiber	10%	20%	30%	40%	50%
Actual Distance along fiber (cm)	150	300	450	600	750
Sr-90/Y-90 Beta					
Rep 1	166.6	304.2	454.6	601.5	753
Rep 2	164.7	304.6	456.5	602.3	753.5
Rep 3	164.3	306.2	455.9	603.9	755.5
AVERAGE	165.2	305.0	455.7	602.6	754.0
STDEV	1.2	1.1	1.0	1.2	1.3
Cs-137 Gamma					
Rep 1	159.2	303.7	451.9	601.7	754.6
Rep 2	161.5	303.9	453.8	601.2	753.9
Rep 3	161.0	302.6	451.5	603.7	755.4
AVERAGE	160.6	303.4	452.4	602.2	754.6
STDEV	1.2	0.7	1.2	1.3	0.8

Additionally, two collimated sources were placed close together along the fiber to determine whether they can be resolved as two peaks at nominal distances along the fiber (**Table 4**). The distance between the two sources was successively reduced in 5 cm increments until the peaks were no longer resolved. The experiments were repeated in triplicate, with the shortest distance between the two sources reported in centimeters for each experiment. Since the Am-241 source is not detectable with the 10-m fiber, the measurement with Cs-137 and Am-241 has no results. The criteria for peaks to be resolved was a dip between the two peaks of approximately 25% of the maximum of the smaller of the two peaks. An example is shown in **Figure 14**. This criterion is similar to the Rayleigh criteria used to define the distance needed for two point sources to be resolved optically. Since the position resolution is dominated by the timing of the system, which does not change with the various measurements, it is not surprising that all results are the same.

Table 4. Two-Source Resolution Test Matrix with Replicates in Parentheses for a 10-m Seven-Fiber Bundle

Source / Radiation					
Nominal Distance along fiber	10%	20%	30%	40%	50%
Actual Distance along fiber (cm)	100	200	300	400	500
Cs-137 + Sr-90/Y-90					
Rep 1	50	50	50	50	50
Rep 2	50	50	50	50	50
Rep 3	50	50	50	50	50
AVERAGE	50	50	50	50	50
STDEV	0	0	0	0	0
Cs-137 + Co-60					
Rep 1	50	50	50	50	50
Rep 2	50	50	50	50	50
Rep 3	50	50	50	50	50
AVERAGE	50	50	50	50	50
STDEV	0	0	0	0	0
Cs-137 + Am-241	NO RESULTS				

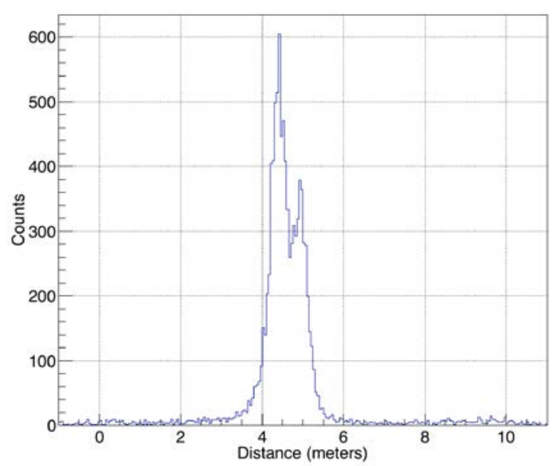

Figure 14. Example Plot Showing Two Sources, Cs-137 and Co-60, Located 50 cm Apart.

3.2.3 Dose Rate Accuracy

To test the dose rate accuracy of the PSF detector, the dose rate from radioisotope sources was first measured using a handheld dose rate meter. The source was then measured at several different locations along the seven-fiber bundle using the PSF detector and different distances from the seven-fiber bundle to ensure that the PSF dose rate reading is consistent with the handheld dose rate meter. An experimental test matrix for determining dose rate accuracy is shown in **Table 5**, which details the conditions at which dose rate accuracy was measured. These measurements were all taken with the detector in air. The percent values refer to the position along the fiber or fiber bundle where the measurement was taken. Low, Medium, and High refer to three different dose rates that were measured. The actual values were different for the different gamma and beta measurements. Low dose rates were determined to be near the low end of detection for the system. High dose rates were determined to be either near the highest dose rate the system can measure or as high as could be obtained with available sources. Medium was designated to be a dose rate between High and Low. The High, Medium and Low values were determined after the characteristics of the system were known. The test matrix was completed by comparing the dose rate measured on the hand-held survey meter and the dose rate measured using the seven-fiber bundle PSF detector.

The bundle was calibrated using a Cs-137 gamma source because its energy is near the middle of the energy spectrum. Different calibration coefficients are used for different positions along the fiber since varying amounts of light loss occur due to fiber attenuation. The fiber was curved around the point sources used to try to expose them to a consistent radiation field which improves measurement accuracy. The results indicate that the system is insensitive to gamma rays below approximately 150 keV since 59.5 keV gammas from Am-241 were not detected at all, and 122 keV gammas from Co-57 produced dose rates significantly lower than what was actually present. Similarly, low dose rate results were measured for the Cs-137 beta particles, which have a relatively low-end point energy of 514 keV. The system clearly responds to them as seen below. The response is not due solely to gammas because the dose rate drops significantly when a thin piece of plastic is inserted between the Cs-137 beta source and the fiber.

The beta dose rate will read too low for at least two reasons. First, the betas slow down or stop in the heat shrink tube that surrounds the fibers, which reduces the energy deposited in the fibers and hence their dose. Second, the betas also slow down or stop in the fibers closest to the source, which makes the active volume smaller than the total volume. Since dose and dose rate are based on mass, the measured dose rate will be less than the actual dose rate.

Table 5. Dose Rate Accuracy Test Matrix for a 10-m Seven-Fiber Bundle. Dose rates are in microrem (μr) per h

Nominal Distance along fiber	10%	30%	50%	10%	30%	50%	10%	30%	50%
Actual Distance Along Fiber (cm)	100	300	500	100	300	500	100	300	500
Nominal Dose Rate	Low	Low	Low	Medium	Medium	Medium	High	High	High
Cs-137 Beta	130	130	130	430	430	430	1800	1800	1800
Rep 1	31	33	28	44	59	59	112	196	167
Rep 2	35	25	32	50	53	60	97	186	181
Rep 3	30	34	40	54	63	62	110	188	192
AVERAGE	32.00	30.67	33.33	49.33	58.33	60.33	106.33	190.00	180.00
STDEV	2.65	4.93	6.11	5.03	5.03	1.53	8.14	5.29	12.53
Sr-90/Y-90 Beta	120	120	120	470	470	470	1650	1650	1650
Rep 1	50	70	122	330	283	531	852	783	1164
Rep 2	52	88	104	327	275	441	834	830	1049
Rep 3	49	65	90	341	279	420	738	832	965
AVERAGE	50.33	74.33	105.33	332.67	279.00	464.00	808.00	815.00	1059.33
STDEV	1.53	12.10	16.04	7.37	4.00	58.97	61.29	27.73	99.90
Am-241 Gamma	NO RESULTS								
Co-57 Gamma	60	60	60	120	120	120	220	220	220
Rep 1	17	24	33	19	22	24	30	48	40
Rep 2	18	35	31	21	23	34	41	44	44
Rep 3	16	21	30	19	24	38	32	46	40
AVERAGE	17.00	26.67	31.33	19.67	23.00	32.00	34.33	46.00	41.33
STDEV	1.00	7.37	1.53	1.15	1.00	7.21	5.86	2.00	2.31
Cs-137 Gamma	50	50	50	220	220	220	530	530	530
Rep 1	43	47	63	225	217	221	408	396	496
Rep 2	44	44	61	218	223	205	444	402	528
Rep 3	49	47	59	230	198	202	437	407	547
AVERAGE	45.33	46.00	61.00	224.33	212.67	209.33	429.67	401.67	523.67
STDEV	3.21	1.73	2.00	6.03	13.05	10.21	19.09	5.51	25.77
Co-60 Gamma	60	60	60	130	130	130	880	880	880
Rep 1	58	61	72	224	168	157	676	841	797
Rep 2	53	57	62	232	175	183	673	903	679
Rep 3	52	56	63	244	176	178	630	730	805
AVERAGE	54.33	58.00	65.67	233.33	173.00	172.67	659.67	824.67	760.33
STDEV	3.21	2.65	5.51	10.07	4.36	13.80	25.74	87.65	70.55
Ba-133 Gamma	50	50	50	100	100	100	270	270	270
Rep 1	23	26	25	41	42	40	111	144	142
Rep 2	25	27	26	46	46	33	133	150	139
Rep 3	23	23	24	42	50	41	117	128	131
AVERAGE	23.67	25.33	25.00	43.00	46.00	38.00	120.33	140.67	137.33
STDEV	1.15	2.08	1.00	2.65	4.00	4.36	11.37	11.37	5.69

No Source (blank control)	15	15	15						
Rep 1	14	15	13						
Rep 2	15	17	10						
Rep 3	18	13	16						
AVERAGE	15.67	15.00	13.00						
STDEV	2.08	2.00	3.00						

3.2.4 Minimum Detectable Dose Rate

To evaluate the minimum dose rate that can be measured by the PSF detector, the distance between the source and the seven-fiber bundle was increased until no statistically significant signal was observed. Longer integration times can yield lower minimum detectable dose rates. All measurements for determining minimum detectable dose rates were made for 10 seconds. Several locations along the bundle were measured. The minimum detectable dose rate did not vary much by location along the fiber.

The matrix shown in **Table 6** identifies the positions and isotopes that were used to measure the minimum detectable dose rate. The position is listed as percent of the length of the bundle being tested. Note that minimum detection limits change based on the radioactive background during the measurement. Background can change based on location (concrete buildings typically have a higher background from K-40) as well as radon concentration (which varies based on weather and other conditions). The test matrix was completed by comparing the dose rate measured on the hand-held survey meter and the seven-fiber bundle until one or both signals fall to background levels.

Table 6. Minimum Detectable Dose Rate Test Matrix with Replicates in Parentheses for 10-m Seven-Fiber Bundle. Dose rates are in μr/h

Nominal Distance along fiber	10%	30%	50%
Actual Distance along fiber (cm)	100	300	500
Cs-137 Beta Dose Rate from Fluke	370	370	370
Rep 1	41	43	35
Rep 2	37	35	35
Rep 3	39	36	40
AVERAGE	39.00	38.00	36.67
STDEV	2.00	4.36	2.89
Am-241 Gamma	NO RESULTS		
Co-57 Gamma Dose Rate from Fluke	30	30	30
Rep 1	37	19	25
Rep 2	26	33	23
Rep 3	25	28	27
AVERAGE	29.33	26.67	25.00
STDEV	6.66	7.09	2.00
Cs-137 Gamma Dose Rate from Fluke	25	25	25
Rep 1	31	47	52
Rep 2	27	38	61
Rep 3	42	35	41
AVERAGE	33.33	40.00	51.33
STDEV	7.77	6.24	10.02
Co-60 Gamma Dose Rate from Fluke	25	25	25
Rep 1	34	49	33
Rep 2	56	45	38
Rep 3	44	37	29
AVERAGE	44.67	43.67	33.33
STDEV	11.02	6.11	4.51

3.2.5 Transportation and Water Infrastructure Applications

The results garnered from experiments described in Sections 3.3 to 3.5 were used to determine the operating parameters for demonstration of the LLNL-developed prototype PSF detector to measure contamination and dose rates on surfaces (such as roads or soil).

Additional experiments were performed to determine the speed at which a bundled fiber detector can be moved over a surface to scan for contamination while maintaining a detectable signal.

In conjunction with measurements taken with the fiber placed under water, an assessment was made of the detection properties of the bundled fiber detector to measure dose through water. Specifically, a portion of the 10-m seven-fiber bundle was placed under water and gamma sources were placed in air, next to the water container.

To evaluate the minimum dose rate that can be measured by the PSF detector while it is submerged, the distance between the source and the seven-fiber bundle was increased until no statistically significant signal was observed. Longer integration times can yield lower minimum detectable dose rates. Results in **Table 7** are for 10 second counts. For Co-57, longer integration times were tried, but there was still no signal with water between the source and the fiber.

The matrix shown in **Table 7** identifies the isotopes that were used to measure the minimum detectable dose rate. Note that minimum detection limits change based on the radioactive background during the measurement. Background can change based on location (concrete buildings typically have a higher background from K-40) as well as radon concentration (which varies based on weather and other conditions). The test matrix was completed by measuring the dose rate using the seven-fiber bundle until the signal falls to background levels.

A measurement was made using a Sr-90 source. As expected, even 1 cm of water blocks essentially all betas.

Table 7. Minimum Detectable Dose Rate Test Matrix with Replicates in Parentheses for a Submerged Portion of 10-m Seven-Fiber Bundle in Water

	Min. Det. Dose Rate
Am-241 Gamma	NO RESULTS
Co-57 Gamma	NO RESULTS
Cs-137 Gamma Dose Rate by Fluke	80
Rep 1	70
Rep 2	52
Rep 3	37
AVERAGE	53
STDEV	16.5
Co-60 Gamma Dose rate by Fluke	60
Rep 1	27
Rep 2	41
Rep 3	49
AVERAGE	39
STDEV	11.1

By assessing the characteristics of the seven-fiber bundle in air and measuring the dose rates while the fiber is submerged in water, an assessment can be made regarding the efficiency of the detector in water and the feasibility for water infrastructure applications.

3.3 Quality Assurance and Quality Control

The dose rate meter was checked before each use to verify there are no errors, that the battery was not low, and that the meter had been calibrated within 1 year. The meter was certified to measure dose rate within 10% when measuring a value that is between 10% and 100% of the full-scale range being used. Full scale ranges available, in mr/h, are 5, 50, 500, 5000, and 50000. The meter was recalibrated annually by the LLNL Environmental Safety and Health Functional

Area. The calibration is only certified for x-ray and gamma radiation between 20 keV and 2 MeV. The meter also responds to beta radiation, but is not certified to 10% error.

4. Conclusions and Recommendations

This study evaluated the potential use of PSF detection system during a wide area radiological incident response. A prototype PSF system was developed and characterized. The cost of a prototype PSF system is relatively inexpensive (less than $5k) compared to other mobile survey methods described in Section 1. Comparative sodium iodide equipment costs range from $5k to $40k each, but such a system does not offer the positioning sensitivity that PSF provides. The operating guide for the prototype PSF is in **Appendix A**.

The 10-m fiber bundle can be a very useful tool for decontamination or monitoring missions. Using a bundle of seven 2 mm diameter fibers, the system is sensitive to typical background dose rates for gamma rays using a 1 second integration time. Point sources can be located within 5 cm along the fiber length by measuring the difference in arrival time of light from interactions. The system can detect a 10 µCi Co-60 source or a 40 µCi Cs-137 source at 1 m in a few seconds. If used on a vehicle with the fiber mounted on a boom within 20 cm of the ground, the system could detect these sources while traveling at 2 mph. By using a thin cladding material such as heat shrink tubing, the system can be sensitive to beta decays as well, which is beneficial for monitoring for contamination.

The 15-m fiber that was tested demonstrated that the attenuation along the fiber is too great to allow good performance. In the future, a lower attenuation fiber could be used to increase the fiber length, if desired. A lower attenuation fiber would also improve the performance of a 10-m bundle by improving its low energy performance. Note that the quantum efficiency of PMTs drops quickly at longer wavelengths, so moving to a green-emitting fiber with lower attenuation will likely result in poorer overall performance. With the current 10-m fiber bundle, many of the detected events had only a single photon detected at one of the PMTs, especially for lower energy sources, making PMT selection critical as well.

The oscilloscope used in this system, the DRS4 demonstration board, has several limitations. The two most significant limitations are a count rate limit of approximately 500 counts per second, and a limited ability to define what constitutes a coincidence. The count rate limit is not a problem in relatively low dose rate environments, up to several mr/h. Higher dose rate environments could be accommodated by accounting for dead time. The limitations on the trigger will make it difficult to use on fibers longer than approximately 15 m.

Future development of the system could focus on several areas. First, using Kurary fibers with a 4-m attenuation length would improve the performance of 10 m fibers and would allow longer fibers to be used, probably to approximately 20 m. We were not able to obtain Kurary fibers for testing in this project. Other methods to increase the fiber length include having multiple sections back to back (this requires PMTs along the length of the fiber, which could be cumbersome), or having multiple shorter segments of scintillating fiber connected to non-scintillating plastic or silica fiber. Non-scintillating fibers can have attenuation lengths orders of magnitude longer than scintillating fibers, so very long fibers would be possible. The ultimate length would be limited by count rates; to determine the location of an event, it must be unlikely that pulses not from that event (such as dark counts from the PMT or a second event) occur at the same time, causing a random coincidence.

If a large number of these systems are required, then a manufacturing prototype could be developed in coordination with a company to segue into larger scale production.

Another area for future studies would be algorithm development. The system is clearly sensitive to low levels of radioactivity, but the performance could be improved by developing algorithms to statistically determine if a location along the fiber is above background. This development would also make the system considerably easier to use for an operator. While these types of algorithms exist in general, they would need to be applied to this specific application. The unique characteristics of the system could be used to advantage as well. For example, sections of the fiber not near contamination could be used to determine background in real time, thus improving minimum detection levels.

The system should also be integrated with a global positioning system (GPS) to determine the geolocations of the fiber end points, allowing the dose rates along the fiber to be encoded with latitude and longitude coordinates. This GPS could be integrated into a GIS system to make maps or into a more advanced (or existing) system to provide situational awareness.

Finally, since the basic hardware design has been shown to be effective, the actual use cases could be expanded. Mounting the fiber on a boom in front of a vehicle to monitor a road or field is an obvious use. Monitoring fixed locations such as water infrastructure is another possibility. One could imagine a swarm of tethered balloons (or unmanned aerial vehicles) with fibers dangling below to monitor a radioactive plume moving through the atmosphere. Many other possibilities exist.

5. References

Berlman, I.B. (1971) *Handbook of Fluorescence Spectra of Aromatic Molecules*. New York: Academic.

Burmeister, H., Sonderegger, P., Gago, J.M., Maio, A., Pimenta, M., Perrin, D. and Thevenin, J.C. (1984) *Electromagnetic Calorimetry using Scintillating Plastic Fibres*, Nuclear Instruments and Methods in Physics Research, 225:530-533.

Chichester, D.L., Watson, S.M. and Johnson, J.T. (2012) *Comparison of BCF-10, BCF-12 and BCF-20 Scintillating Fibers for use in a 1-Dimensional Linear Sensor*, IEEE Nuclear Science Symposium 2012. Also available as an Idaho National Laboratory Report, INL/CON-12-25807, October 2012.

Chupp, E.L. and Forrest, D.J. (1966) *A Directional Neutron Detector for Space Research Use*, IEEE Transactions on Nuclear Science, 13(1):468-477.

DHS (2013) *Standoff Radiation Detectors: Market Survey Report*, Department of Homeland Security (DHS) Report, August 2013, National Urban Security Technology Laboratory.

Gamo, H., Kondo, M., Hashimoto, T., Tayama, R. and Tsukiyama, T. (2014) *Development of a PSF-Detector for Contaminated Areas*, Progress in Nuclear Science and Technology, 4:695-698.

GAO (2013) *Nuclear Terrorism Response Plans: Major Cities Could Benefit from Federal Guidance on Responding to Nuclear and Radiological Attacks*, Report GAO-13-736, US Government Accountability Office, Washington, DC. (September 2013).

Imai, S-I., Soramoto, S., Mochiki, K-I. and Iguchi, T. (1991) *New Radiation Detector of Plastic Scintillation Fiber*, Review of Scientific Instruments, 1991, 62(4):1093-1097.

Ishikawa, M., Unesaki, N., Kobayashi, T., Sakurai, Y., Tanaka, K, Endo, S., Hoshi, M. (2002) *Real-Time Estimation of Neutron Flux During BNCT treatment using Plastic Scintillation Detector with Optical Fiber*, 10th International Congress on Neutron Capture Therapy, Essen, Germany, September 2002, published in Research and Development in Neutron Capture Therapy, pp443-447.

JAEA (2011) *Fukushima Support Headquarters News*, No. 3, Japan Atomic Energy Agency (JAEA) October 14th, 2011 (Japanese).

JAEA (2014a) *TOPICS Fukushima*, Japan Atomic Energy Agency (JAEA) Aug 8th 2014, No. 50, available at: http://fukushima.jaea.go.jp/english/topics/pdf/topics-fukushima050e.pdf (accessed October 2017).

JAEA (2014b) *TOPICS Fukushima*, Japan Atomic Energy Agency (JAEA) Oct 10th 2014, No. 53, available at: http://fukushima.jaea.go.jp/english/topics/pdf/topics-fukushima053e.pdf (accessed October 2017).

JAEA (2015) *TOPICS Fukushima*, Japan Atomic Energy Agency (JAEA) Feb 20th 2015, No. 61, available at: http://fukushima.jaea.go.jp/english/topics/pdf/topics-fukushima061e.pdf (accessed October 2017).

Jopson, R.C., Wright, R.E and Mark, H. (1960) *Thin Fiber Scintillation Counter for Determining Particle Beam Distributions in Accelerators*, Lawrence Livermore National Laboratory Report UCRL-5818, Livermore CA.

Nohtomi, A., Sugiura, N., Itoh, T. and Torii, T. (2008) *On-line Evaluation of Spatial Dose-Distribution by using a 15m-long Plastic Scintillation-Fiber Detector*, IEEE Nuclear Science Symposium Conference Record, N02-193, 965.

Oka, T., Fukiwara, H., Takashima, K., Isami, T. and Tsutaka, Y. (1998) *Development of Fiber Optic Radiation Monitor using Plastic Scintillation Fibers*, Journal of Nuclear Science and Technology, 35(12):857-864.

Park, J.W. and Kim, G.H. (2004) *Detection of Gamma Rays using Plastic Scintillating Fibers*, Journal of Nuclear Science and Technology, Suppl. 4, 373-376.

Reynolds, G.T. and Condon, P.E. (1957) *Filament Scintillation Counter*, Review of Scientific Instruments, 28:1098-1099.

Ruchti, R.C. (1996) *The Use of Scintillating Fibers for Charged-Particle Tracking*, Annual Reviews of Nuclear and Particle Science, 46:281-319.

Sanada, Y., Urabe, Y., Orita, T., Takamura, Y. and Torii, T. (2015) *In-situ Measurement of Radiation Distribution in Bottom Sediments of Irrigation Ponds using Plastic Scintillation Fiber*, Proceedings of the 23rd International Conference on Nuclear Engineering, Chiba, Japan, May 17-21, 2015.

Takasaki, F., Saito, H., Shimizu, T., Kondo, S. and Shinji. O. (1987) *Development of Plastic Scintillation Fiber*, Nuclear Instruments and Methods in Physics Research, A262: 224-228.

Todani, K. (2011) *JAEA Activities Towards Environmental Restoration of Fukushima*, Japan Atomic Energy Agency (JAEA) Report, Headquarters of Fukushima Partnership Operations, October 16th, 2011, available at: http://www.jaea.go.jp/fukushima/pdf/decon_e_09.pdf (Japanese) (accessed October 2017).

Torii, T. and Sanada, Y. (2013) *Measurement Technology of Pollution Distribution Taken in a Plane*, Isotope News, No. 714, October 2013 (Japanese).

Appendix A: Prototype PSF Operating Guide

A.1 Components and System Description

The major components of the system are the fiber, PMTs, a DRS4 digital oscilloscope, Raspberry Pi single board computer, and Samsung Galaxy Tab S2 tablet. Everything is powered from a USB battery pack that supplies 5 volts to the Raspberry Pi.

Saint Gobain BCF-12 plastic scintillating fibers were used. The fast decay time (3.2 ns) allows for accurate location determination by measuring the difference in time of arrival of the light from an event at the two PMTs. The attenuation length of 2.7 m allows the use of fibers up to approximately 10 m in length while still maintaining good sensitivity. The double-clad version of the fiber is used to increase the light trapping efficiency. A bundle of seven 2-mm diameter fibers is used to increase the sensitivity to gamma rays. The bundle is enclosed in heat shrink tubing to prevent light from getting to the fibers. The tubing is thin enough to allow beta particles to be detected by the system.

Hamamatsu 10721P-210 PMT modules are used. The modules require only 5 volts to operate, obtained from a USB port on the Pi. The high voltage for the PMTs is provided by the PMT modules and set using potentiometers inside the PMT mounting boxes. The voltages have been set, and it is not recommended to change them. For users experienced with electronics, the PMT supplies 1.2 volts on the blue line as a reference, and the potentiometers are used to supply a voltage between 0 and 1.1 volts to the PMT on the white line, which sets the HV. Do not set the voltage to greater than 1.1 volts. Do not operate the PMTs while exposed to light as permanent damage will result. These modules were selected due to their high quantum efficiency and very low dark count rate, both of which are important due to the small signals generated at the ends of a long fiber.

The DRS4 demonstration board is a four-channel oscilloscope capable of sampling at 5 Giga-samples per second (GSPSs), although this system uses it at 4 GSPSs. The high sampling rate is critical to accurately determine the location of an interaction. The software to run the oscilloscope is available at the DRS4 website: https://www.psi.ch/drs/software-download (last accessed October 2017). The data acquisition is based on version 5.0.6. The make file has been modified to remove the requirement for wxWdigets, which is not used on the current system. One limitation of the DRS4 demo board is a maximum count rate of approximately 500 counts per second. This rate can be exceeded with sources greater than approximately 100 µCi, and the dose rate response would then become non-linear. This limitation could be compensated for in future versions, or a different hardware solution could be used.

The Raspberry Pi 3 is a very common single board computer. The operating system is run from a microSD card. The usual operating system is Raspian, a variant of Linux based on Debian Linux. The Raspberry Pi 3 has on board WiFi, which is utilized here to communicate with a tablet (the Pi acts as an access point). It also has four USB ports and an HDMI port for a monitor. With a keyboard, mouse, and monitor connected to it, the Pi acts like any other computer.

Power is from a USB battery pack. This battery pack requires a push of a button before providing power. Any USB battery pack should work. The current pack provides approximately eight hours of operation. Note that the battery pack cannot charge and provide power at the same time.
The tablet is a Samsung Galaxy Tab S2 running Android. Other Android tablets should work as well. Android versions between 4.4 and 6 are required for the EPAFiber tablet app. It might work with version 7 of Android but has not been tested.

A.2 Operation

NOTE: The PMTs can be damaged permanently if power is supplied while the PMT is exposed to ambient light. Ensure fibers are connected to both PMTs before supplying their 5 volt lines. Direct exposure to sunlight, even while the PMT is not powered, can cause degradation in performance. Additionally, PMTs are sensitive to magnetic fields, so magnets should be kept away.

To turn the system on, first make sure all the necessary connections are made:

- Connect the desired fiber bundle to both PMTs. For the 3-m and 10-m bundles which have wires attached, the side with the short wires goes to PMT2, which is the PMT located away from the rest of the system.
- Connect the 5-volt power to both PMTs, which are provided via cables with BNC connectors. The 5 volts is supplied by a USB to BNC adapter from the Raspberry Pi.
- The signals from the PMTs are transmitted over coax using SubMiniature version A (SMA) connectors. If using the 10-m fiber bundle, use the long (10 m) delay line to connect PMT1 (the PMT closest to the oscilloscope) to channel 1 on the oscilloscope. The delay line is required to allow the oscilloscope to detect coincidences over the entire length of the fiber. For other fibers, use the short (18 inch) SMA cable to connect PMT1 to the DRS4.
- Connect the DRS4 oscilloscope to the Raspberry Pi with a USB cable.
- If desired, the Raspberry Pi can be connected to a keyboard, mouse, and monitor. This connection is useful if collecting data from the system.
- Connect the USB battery pack or wall power supply to the Raspberry Pi. If using the supplied USB battery pack, you must press the button on the battery pack before it supplies power.

The Raspberry Pi is configured to automatically start the data collection software on boot up, which occurs when the Pi gets power. If the DRS4 is not connected to the Pi when the Pi is turned on, the data collection software will quit. Turn on the tablet, which should automatically connect to the WiFi of the Raspberry Pi. On the main page is an app called EPAFiber. Click on the app. Go to the settings tab and select the cable you are using, then click on waterfall to go back. Click on the Start button in the lower left corner and counts should start appearing.

The system occasionally freezes or doesn’t start up properly. The simplest solution is to shut down the Pi, remove power from the Pi for five seconds, and restart the system. More detailed troubleshooting is below.

Saving data from the system is more involved and requires the system be connected to a keyboard, mouse, and monitor. Begin by ensuring the system is connected as above. The Raspberry Pi runs a flavor of Linux, with a graphical user interface which is similar to other operating systems. The actual commands will be entered via a command line in a terminal window. The steps are listed next, with details following:

- The system automatically starts a server process (called server) and data acquisition process (called drs_exam) at startup. Kill these processes for manual data collection.
    - In a command line on the Pi, type ps –ef |grep drs_exam
    - Find the process number of drs_exam (typically about 485)
    - Type sudo kill 485 (or whatever the process number actually is)
- Move to the directory Desktop/epa_standalone.
    - In a command line, type cd Desktop/epa_standalone
- Copy the setting file for the length fiber you are using to the file named DRS_settings.txt.
- Use the command sudo ./drs_exam to acquire data.
- Data are saved in files named rawdata.csv and doserate.csv. If they are not renamed, they will be overwritten.

A terminal window can be opened by clicking on the icon near the top right of the screen. The files we care about are located in the folder /pi/users/pi/Desktop/drs.

Once data are collected in the files rawdata.csv and doserate.csv, they can be renamed using the graphical user interface (or command line if you prefer). Then they can be copied to a USB flash drive for analysis on another computer.

EPA
United States
Environmental Protection
Agency

Office of Research and Development (8101R)
Washington, DC 20460